

DIRECT ERROR BOUNDS FOR SYMMETRIC RBF COLLOCATION

Robert Schaback

Institut für Numerische und Angewandte Mathematik (NAM)
Georg-August-Universität Göttingen
Lotzestrasse 16-18
D-37083 Göttingen
e-mail: schaback@math.uni-goettingen.de,
web page: <http://num.math.uni-goettingen.de/schaback>

Keywords: Meshless, radial basis function, Power Function, greedy methods

Summary. The standard error bounds for interpolation by kernels or radial basis functions are generalized to symmetric PDE collocation problems. This involves generalized Power Functions, and these can be explicitly calculated. Final error bounds then are a product of Power Function values and the norm of the solution in the native space of the kernel. Since the latter can also be estimated well, the whole procedure yields error bounds of the symmetric collocation solution on all points of the domain. Some numerical examples are given for illustration, including a greedy method for choosing good collocation points. On the theoretical side, a short proof of optimal convergence rates for problems with smooth solutions is provided.

1 INTRODUCTION

If a general linear PDE problem of the form

$$\begin{aligned} Lu &= f & \text{in } \Omega \\ Bu &= g & \text{in } \Gamma := \partial\Omega \end{aligned} \tag{1}$$

with a differential operator L and a “boundary” operator B is posed in a bounded domain $\Omega \subset \mathbb{R}^d$, users can collocate both operators at discrete points of Ω and the boundary. Whatever the operators are, the discretized equations take the form

$$\lambda_k(u) = f_k \in \mathbb{R}, \quad 1 \leq k \leq N \tag{2}$$

for functionals λ_k that are of the form $\lambda(u) = (Lu)(\mathbf{x})$ or $\lambda(u) = (Bu)(\mathbf{y})$ for certain points $\mathbf{x} \in \Omega$ or $\mathbf{y} \in \partial\Omega$.

The equations (2) can be posed on a *trial space*, and the resulting linear system, if solvable, provides an approximate solution. If the trial space is not directly related to the functionals, solvability of the system is not guaranteed [7].

However, if users take a reproducing kernel Hilbert space \mathcal{N} of functions on Ω with a smooth positive definite kernel K such that all functionals $\lambda_1, \dots, \lambda_N$ are continuous on \mathcal{N} , the trial space spanned by the functions $u_k(\mathbf{y}) := \lambda_k^{\mathbf{x}} K(\mathbf{x}, \mathbf{y})$ guarantees unique solvability of the system (2). Here and later on, a functional $\lambda^{\mathbf{x}}$ acts with respect to the variable \mathbf{x} . The coefficient matrix has entries $\lambda_j^{\mathbf{y}} \lambda_k^{\mathbf{x}} K(\mathbf{x}, \mathbf{y})$, $1 \leq j, k \leq N$ and is positive definite. This setup goes back to [15] in the form of Hermite–Birkhoff interpolation and has been applied to PDE solving by various authors, e.g. [16] in the context of Computational Mechanics. A variant with fast evaluation is in [8], and the method is treated in detail in the books [1, 14, 3], while a comparison of symmetric and unsymmetric collocation is in [10].

A first convergence proof of the symmetric collocation technique appeared in [4, 5], while a much better convergence analysis is in [6]. We shall provide a simplified version below.

By standard techniques of reproducing kernel Hilbert spaces, the error of an interpolant s to a function u in the Hilbert space \mathcal{N} can be bounded pointwise as

$$|s(\mathbf{x}) - u(\mathbf{x})| \leq P_{\Lambda}(\mathbf{x}) \|u\|_{\mathcal{N}} \quad (3)$$

for all functions $u \in \mathcal{N}$ with the *Power Function*

$$\begin{aligned} P_{\Lambda}(\mathbf{x}) &:= \sup\{u(\mathbf{x}) : u \in \mathcal{N}, \|u\|_{\mathcal{N}} \leq 1, \lambda_k(u) = 0, 1 \leq k \leq N\} \\ &= \inf_{a_k \in \mathbb{R}} \left\| \delta_{\mathbf{x}} - \sum_{k=1}^N a_k \lambda_k \right\|_{\mathcal{N}^*}. \end{aligned} \quad (4)$$

Using standard methods from quadratic optimization and a Lagrange basis u_1, \dots, u_N of the trial space with $\lambda_k(u_j) = \delta_{jk}$, $1 \leq j, k \leq N$, the Power Function can be explicitly evaluated pointwise [12, 14] via

$$P_{\Lambda}^2(\mathbf{x}) = K(\mathbf{x}, \mathbf{x}) - \sum_{k=1}^N u_k(\mathbf{x}) \lambda_k^{\mathbf{y}} K(\mathbf{x}, \mathbf{y}). \quad (5)$$

Following the computational issues in [13], we shall provide some numerical examples in the next section.

The upshot for practical applications lies in the fact that $P_{\Lambda}(\mathbf{x})$ can be evaluated everywhere in the domain and is by (3) an upper bound for the error, but relative to a multiplicative factor of the true solution. If $\|u^*\|_{\mathcal{N}}$ were known, (3) would provide a full error bound at reasonable cost. In demonstrations of numerical methods, one can take problems with known solutions and then evaluate the quality of the error bound (3) directly. In general, one can take $\|s\|_{\mathcal{N}}$ instead of $\|u^*\|_{\mathcal{N}}$. This quantity is numerically available and usually a good approximation of $\|u^*\|_{\mathcal{N}}$, but always from below, unfortunately.

Anyway, the Power Function tells us where to expect large errors, and where errors will be relatively small due to having enough meshless data there. We shall show in the next section how to interpret plots of the Power Function.

2 EXAMPLES

As a warm-up, let us start with the Poisson equation on the square $[-1, 1]^2$ with Dirichlet boundary conditions for $y = \pm 1$ and Neumann boundary conditions for $x = \pm 1$. We thus have three kinds of functionals when discretizing, and we fix the discretization given in Figure 1. It has 11×11 regular collocation points for the Laplacian, including boundary points, and two sets of 11 points on each boundary line for the Dirichlet and Neumann data.

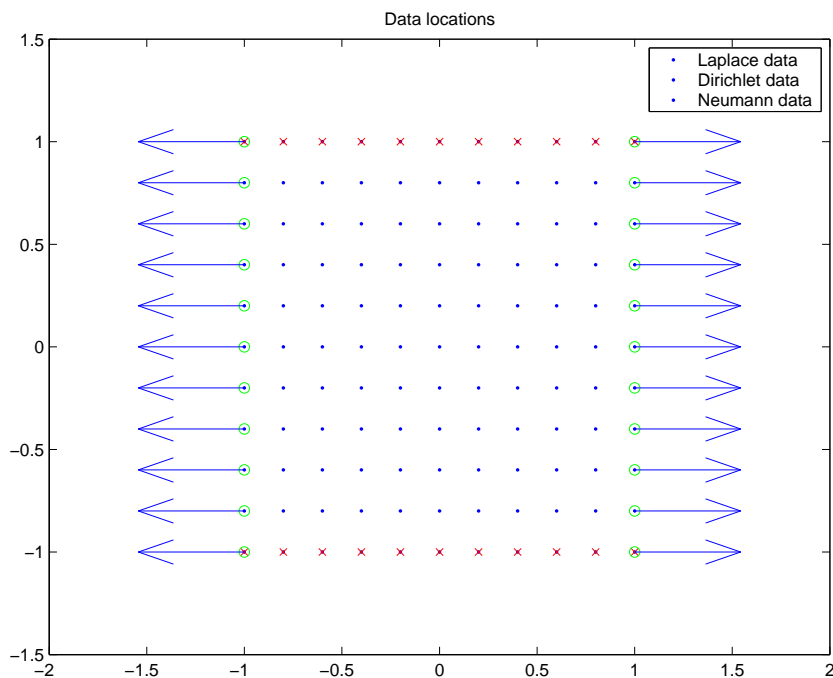


Figure 1: Discretization of Poisson problem

The Power Function for these data, calculated using the Wendland kernel $\phi_{3,4}$ of C^8 smoothness with support radius 10, is in Figure 2. This means that whichever problem is solved on this discretization, the absolute error will be bounded by 0.0016 times the native space norm of the true solution, which in this case is equivalent to the $W_2^{5.5}[-1, 1]^2$ norm. At this point, it should be remarked that the normalization of the kernel and/or the inner product in the native Hilbert space must be properly done. In fact, if the norm in (3) gets a large artificial factor, then the power function gets the inverse factor. We avoided this problem by normalizing the inner product in such a way that the 11×11 interpolant s_G to the Gaussian $G(x, y) = \exp(-x^2 - y^2)$ has native space norm one. Thus the Power Function is in particular a strict error bound for the specific problem with true solution $s_G \approx G$, whichever kernel is taken. Another possibility of normalization is to let the kernel take the value 1 at zero. This leads to similar results.

The Power Function for the Gaussian kernel at scale 0.4 is in Figure 3. For other

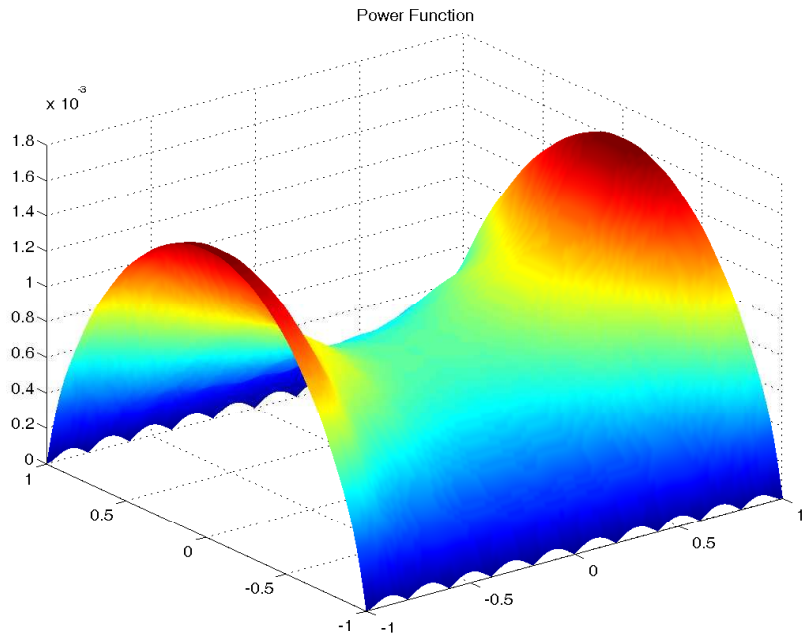


Figure 2: Power Function for C^8 Wendland function, scale 10^{-3} on y axis

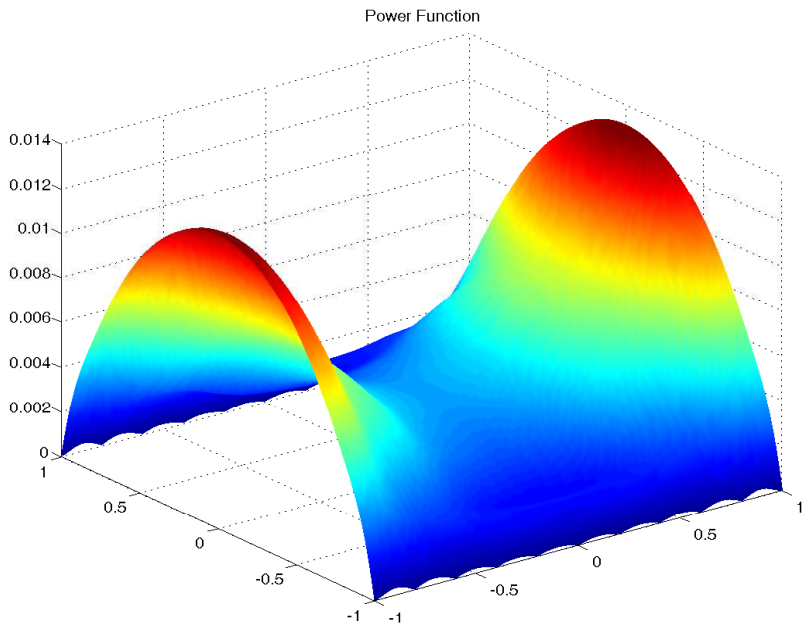


Figure 3: Power Function for Gaussian

kernels, the situation is similar. Inspecting these plots, we see that there are not enough Neumann points, since the Power Function takes its maximum on the Neumann boundary.

The second set of examples works in the unit disc with the third quadrant cut away,

and we pose the Poisson problem with Dirichlet data. On the points in Figure 4 we get the Power Function of Figure 5. Since the maxima are on the boundary, this tells us that we need more boundary points, while keeping the collocation points for the Laplacian. This yields Figures 6 and 7 where there now are interior and boundary maxima at the same level, i.e. there is some equilibrium between boundary and interior data. These plots were done for the Wendland function $\phi_{3,4}$ at scale 5, and results are very similar for other kernels.

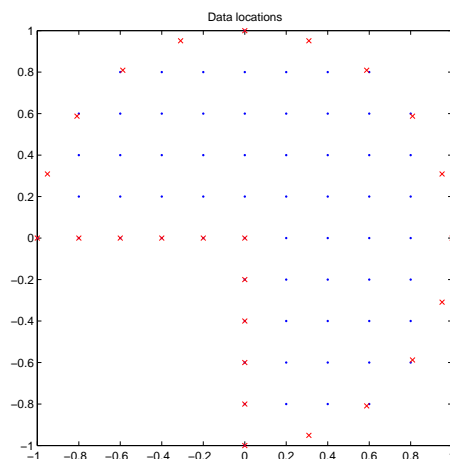


Figure 4: Data Locations for Wendland Function

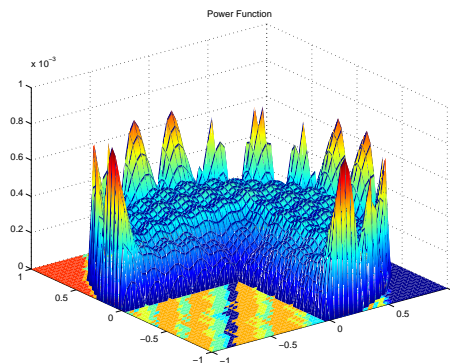


Figure 5: Power Function for Wendland Function

This raises the question of optimal placement of collocation points. In [2], new collocation points are chosen one by one as points where the Power Function attains a maximum. It is tempting to apply this directly to the Power Functions in the preceding plots, but it may happen (and actually happens) that interior maxima of the Power Function occur at collocation points for the Laplacian, and then the method breaks down.

This can be avoided by using the Power Function (4) only on the Dirichlet boundary, and placing new boundary points at extrema of this function. In the interior, the

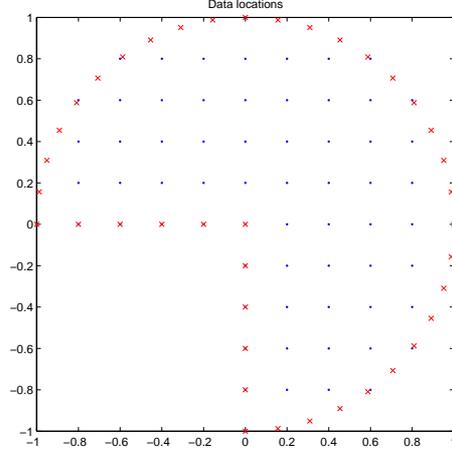


Figure 6: Data Locations for Wendland Function

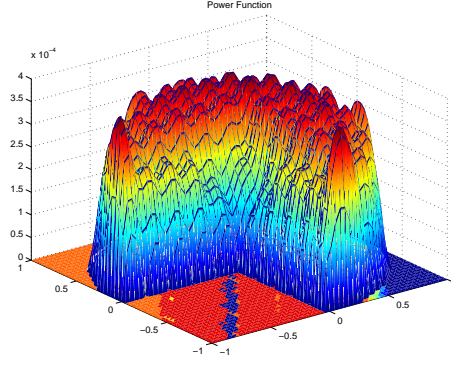


Figure 7: Power Function for Wendland Function

generalized Power Function

$$\begin{aligned}
 P_{\Lambda, \Delta}(\mathbf{x}) &:= \sup\{\Delta u(\mathbf{x}) : u \in \mathcal{N}, \|u\|_{\mathcal{N}} \leq 1, \lambda_k(u) = 0, 1 \leq k \leq N\} \\
 &= \inf_{a_k \in \mathbb{R}} \|\delta_{\mathbf{x}} \circ \Delta - \sum_{k=1}^N a_k \lambda_k\|_{\mathcal{N}^*}.
 \end{aligned} \tag{6}$$

is used, and its maxima are candidates for new collocation points for the Laplacian. Note that in general

$$\begin{aligned}
 &\inf_{a_k \in \mathbb{R}} \|\lambda - \sum_{k=1}^N a_k \lambda_k\|_{\mathcal{N}^*}^2 \\
 &= \inf_{a_k \in \mathbb{R}} \left((\lambda, \lambda)_{\mathcal{N}^*} - 2 \sum_{k=1}^N a_k (\lambda, \lambda_k)_{\mathcal{N}^*} + \sum_{j,k=1}^N a_j a_k (\lambda_j, \lambda_k)_{\mathcal{N}^*} \right)
 \end{aligned} \tag{7}$$

which can be reduced to numerical linear algebra by the standard identity $(\lambda, \mu)_{\mathcal{N}^*} = \lambda^{\mathbf{x}} \mu^{\mathbf{y}} K(\mathbf{x}, \mathbf{y})$ in the dual of a reproducing kernel Hilbert space.

It remains open to choose either an extremal point of P_Λ on the boundary or an extremal point of $P_{\Lambda,\Delta}$ in the domain. We chose extrema of $\max(10 \cdot P_\Lambda, P_{\Lambda,\Delta})$ with the factor 10 being fixed experimentally to get a balance between boundary and interior data. This choice is related to the ratio of the constants in inequalities like

$$\|u\|_\Omega \leq C_{\partial\Omega}\|u\|_{\partial\Omega} + C_\Omega\|\Delta u\|_\Omega \quad (8)$$

describing well-posedness of the Dirichlet problem. The relative size of the two constants describes the relative influence of boundary and interior recovery precision on the actual solution. Figure 8 shows the final result of a run of this greedy algorithm, using the same Wendland function again. It should be finally noted that we always work with smooth

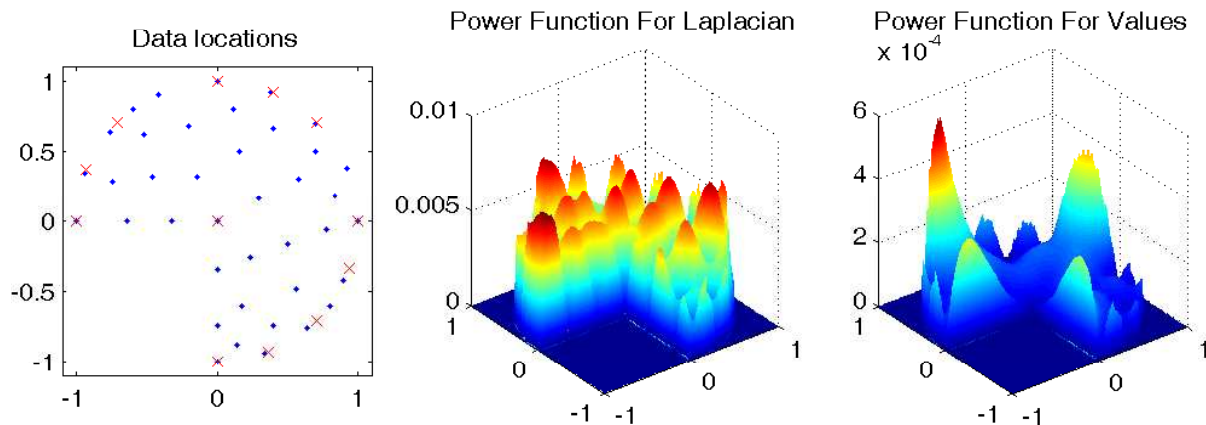


Figure 8: Optimized Power Function for Wendland Function

solutions that lie in native Hilbert spaces of a smooth kernel. This means that there will be no derivative singularities induced by incoming corners, and thus our setting will not deteriorate in the incoming corner. If boundary data are just continuous, the solutions may have derivative singularities and are only in $W_2^1(\Omega)$. This case cannot be handled by the setting in this section, since point evaluation of the Laplacian is not continuous. By choosing other data functionals and other kernels, weak problems can also be treated and Power Functions can be evaluated, using (7). But this is beyond the scope of this paper.

3 ERROR BOUNDS AND CONVERGENCE

For simplicity, we focus on the Dirichlet problem

$$\begin{aligned} \Delta u &= f & \text{in } \Omega \\ u &= g & \text{in } \Gamma := \partial\Omega \end{aligned} \quad (9)$$

for the Poisson equation in a bounded domain $\Omega \subset \mathbb{R}^d$, with well-posedness

$$\|u\|_{k,\Omega} \leq C \left(\|\Delta u\|_{k-2,\Omega} + \|u\|_{k-1/2,\Gamma} \right) \quad (10)$$

in Sobolev norm notation, for $k \geq 2$. We assume the true solution u^* to be in $W_2^m(\Omega)$ for some $f \in W_2^{m-2}(\Omega)$ and $g \in W_2^{m-1/2}(\Gamma)$, $m \geq 2$. Then (10) holds for all $2 \leq k \leq m$.

We use two discrete sets $X_h \subset \Omega$ and $Y_h \subset \Gamma$ for symmetric collocation of f and g , respectively, in a RKHS with a smooth kernel K such that its native space \mathcal{N} is contained in $W_2^m(\Omega)$. The sets should have a *fill distance* h which is the maximum of the separate fill distances

$$\begin{aligned} h_{\Omega, X_h} &:= \sup_{\mathbf{y} \in \Omega} \min_{\mathbf{x}_j \in X_h} \|\mathbf{y} - \mathbf{x}_j\|_2 \\ h_{\Gamma, Y_h} &:= \sup_{\mathbf{z} \in \Gamma} \min_{\mathbf{y}_j \in Y_h} \|\mathbf{z} - \mathbf{y}_j\|_2 \end{aligned} \quad (11)$$

in the interior and on the boundary.

We assume *sampling inequalities* of the form

$$\begin{aligned} \|v\|_{\ell, \Omega} &\leq C(h^{n-\ell} \|v\|_{n, \Omega} + \|v\|_{RMSE, X_h}), \quad 0 \leq \ell \leq n \\ \|v\|_{\ell, \Gamma} &\leq C(h^{n-\ell} \|v\|_{n, \Gamma} + \|v\|_{RMSE, Y_h}), \quad 0 \leq \ell \leq n \end{aligned} \quad (12)$$

in the domain and the boundary, taking discrete root-mean-square norms in the second terms of the right-hand sides. Such inequalities are proven in [9], and are treated in more generality in [11]. They hold for sufficiently small h in a sense that we do not want to explain in detail here. But to make the discrete norms on the right-hand side meaningful, these inequalities require point evaluation to be continuous, i.e. $n > d/2$ in the first and $n > (d-1)/2$ in the second case.

The true solution of the problem should be in \mathcal{N} . This implies

$$\|\hat{u}\|_{\mathcal{N}} \leq \|u^*\|_{\mathcal{N}} \quad (13)$$

for the (existing) collocation solution $\hat{u} \in \mathcal{N}$.

Then we use (10) and (12) to get

$$\begin{aligned} \|u^* - \hat{u}\|_{k, \Omega} &\leq C \left(\|\Delta u^* - \Delta \hat{u}\|_{k-2, \Omega} + \|u^* - \hat{u}\|_{k-1/2, \Gamma} \right) \\ &\leq C(h^{m-k} \|\Delta u^* - \Delta \hat{u}\|_{m-2, \Omega} + \|\Delta u^* - \Delta \hat{u}\|_{RMSE, X_h}) \\ &\quad + C(h^{m-k} \|u^* - \hat{u}\|_{m-1/2, \Gamma} + \|u^* - \hat{u}\|_{RMSE, Y_h}) \\ &\leq Ch^{m-k} (\|\Delta u^* - \Delta \hat{u}\|_{m-2, \Omega} + \|u^* - \hat{u}\|_{m-1/2, \Gamma}) \end{aligned} \quad (14)$$

since the discrete terms vanish due to collocation. The choice of $n = m-2$ in the first case requires $n > d/2$, and this means $m > 2 + d/2$. With (13) and Sobolev embedding we can conclude that the norms in the right-hand side are uniformly bounded independent of h . This proves a convergence rate of order $m-k$ in the k -norm for $0 \leq k \leq m > 2 + d/2$, which is an optimal rate.

Theorem 1 *Consider the symmetric collocation method for Poisson problems with Dirichlet data in d variables with a smooth solution $u^* \in W_2^m(\Omega)$, based on a kernel whose native space is contained in $W_2^m(\Omega)$, and with $m > 2 + d/2$. Then, if collocation is done on point sets of fill distance at most h , the convergence is of the form $\mathcal{O}(h^{m-k})$ for $h \rightarrow 0$ in the Sobolev k -norm for $0 \leq k \leq m$.*

It should be clear how this proof pattern generalizes to other situations. Note that we did not use ellipticity, but well-posedness, and note the crucial rôle of sampling inequalities in the argument.

REFERENCES

- [1] M.D. Buhmann. *Radial Basis Functions, Theory and Implementations*. Cambridge University Press, 2003.
- [2] Stefano De Marchi, R. Schaback, and H. Wendland. Near-optimal data-independent point locations for radial basis function interpolation. *Adv. Comput. Math.*, 23(3):317–330, 2005.
- [3] G. F. Fasshauer. *Meshfree Approximation Methods with MATLAB*, volume 6 of *Interdisciplinary Mathematical Sciences*. World Scientific Publishers, Singapore, 2007.
- [4] C. Franke and R. Schaback. Convergence order estimates of meshless collocation methods using radial basis functions. *Advances in Computational Mathematics*, 8:381–399, 1998.
- [5] C. Franke and R. Schaback. Solving partial differential equations by collocation using radial basis functions. *Appl. Math. Comp.*, 93:73–82, 1998.
- [6] P. Giesl and H. Wendland. Meshless collocation: Error estimates with application to dynamical systems. *SIAM Journal on Numerical Analysis*, 45:1723–1741, 2007.
- [7] Y.C. Hon and R. Schaback. On unsymmetric collocation by radial basis functions. *J. Appl. Math. Comp.*, 119:177–186, 2001.
- [8] Michael J. Johnson. A symmetric collocation method with fast evaluation. *IMA J. Numer. Anal.*, 29:773–789, 2009. doi: 10.1093/imanum/drm046.
- [9] W. R. Madych. An estimate for multivariate interpolation. II. *J. Approx. Theory*, 142(2):116–128, 2006.
- [10] H. Power and V. Barraco. A comparison analysis between unsymmetric and symmetric radial basis function collocation methods for the numerical solution of partial differential equations. *Computers and Mathematics with Applications*, 43:551–583, 2002.
- [11] C. Rieger, B. Zwicknagl, and R. Schaback. Sampling and stability. In M. Dæhlen, M.S. Floater, T. Lyche, J.-L. Merrien, K. Mørken, and L.L. Schumaker, editors, *Mathematical Methods for Curves and Surfaces*, volume 5862 of *Lecture Notes in Computer Science*, pages 347–369, 2010.

- [12] R. Schaback. Reconstruction of multivariate functions from scattered data. Manuscript, available via <http://www.num.math.uni-goettingen.de/schaback/research/group.html>, 1997.
- [13] R. Schaback. Matlab programming for kernel-based methods. Technical report, 2009-. Preprint Göttingen, available via <http://num.math.uni-goettingen.de/schaback/research/papers/MPfKBM.pdf>.
- [14] H. Wendland. *Scattered Data Approximation*. Cambridge University Press, 2005.
- [15] Z. Wu. Hermite–Birkhoff interpolation of scattered data by radial basis functions. *Approximation Theory and its Applications*, 8/2:1–10, 1992.
- [16] X. Zhang, K.Z. Song, M.W. Lu, and X. Liu. Meshless methods based on collocation with radial basis functions. *Computational Mechanics*, 26:333–343, 2000. DOI: 10.1007/s004660000181.